

3-4-2022

## Evidence for Paracrine Protective Role of Exogenous $\alpha$ A-Crystallin in Retinal Ganglion Cells

Madhu Nath

Zachary B Sluzala


Ashutosh S Phadte

Yang Shan

Angela M Myers

*See next page for additional authors*

Follow this and additional works at: <https://jdc.jefferson.edu/bmpfp>

 Part of the [Medical Biochemistry Commons](#), and the [Medical Molecular Biology Commons](#)

**[Let us know how access to this document benefits you](#)**

---

This Article is brought to you for free and open access by the Jefferson Digital Commons. The Jefferson Digital Commons is a service of Thomas Jefferson University's [Center for Teaching and Learning \(CTL\)](#). The Commons is a showcase for Jefferson books and journals, peer-reviewed scholarly publications, unique historical collections from the University archives, and teaching tools. The Jefferson Digital Commons allows researchers and interested readers anywhere in the world to learn about and keep up to date with Jefferson scholarship. This article has been accepted for inclusion in Department of Biochemistry and Molecular Biology Faculty Papers by an authorized administrator of the Jefferson Digital Commons. For more information, please contact: [JeffersonDigitalCommons@jefferson.edu](mailto:JeffersonDigitalCommons@jefferson.edu).

---

**Authors**

Madhu Nath, Zachary B Sluzala, Ashutosh S Phadte, Yang Shan, Angela M Myers, and Patrice E Fort

---

---

*Research Article: New Research | Disorders of the Nervous System*

## Evidence for Paracrine Protective Role of Exogenous $\alpha$ A-Crystallin in Retinal Ganglion Cells

<https://doi.org/10.1523/ENEURO.0045-22.2022>

**Cite as:** eNeuro 2022; 10.1523/ENEURO.0045-22.2022

Received: 28 January 2022

Accepted: 2 February 2022

---

*This Early Release article has been peer-reviewed and accepted, but has not been through the composition and copyediting processes. The final version may differ slightly in style or formatting and will contain links to any extended data.*

**Alerts:** Sign up at [www.eneuro.org/alerts](http://www.eneuro.org/alerts) to receive customized email alerts when the fully formatted version of this article is published.

Copyright © 2022 Nath et al.

This is an open-access article distributed under the terms of the Creative Commons Attribution 4.0 International license, which permits unrestricted use, distribution and reproduction in any medium provided that the original work is properly attributed.

1 **Evidence for Paracrine Protective Role of Exogenous  $\alpha$ A-Crystallin in Retinal**  
2 **Ganglion Cells**

- 3 **1. Exogenous  $\alpha$ A-crystallin in retinal neuroprotection**  
4 **2. Madhu Nath<sup>1\*</sup>, Zachary B. Sluzala<sup>1\*</sup>, Ashutosh S. Phadte<sup>1,2\*</sup>, Yang Shan<sup>1</sup>, Angela M.**  
5 **Myers<sup>1</sup>, and Patrice E Fort<sup>1,3</sup>**

6 <sup>1</sup>Department of Ophthalmology and Visual Sciences, University of Michigan, Ann Arbor,  
7 Michigan, USA. <sup>2</sup>Currently in Department of Biochemistry and Molecular Biology, Thomas  
8 Jefferson University, Philadelphia, Pennsylvania, <sup>3</sup>Department of Molecular and Integrative  
9 Physiology, University of Michigan, Ann Arbor, Michigan, USA.

10 \*These authors should be viewed as equal contributors and co-first authors.

11  
12 **3. Designed research, PEF; Performed research, MN, AP, ZBS, YS and AM; Contributed**  
13 **unpublished reagents/ analytic tools, PEF and AM; Analyzed data, PEF, MN, AP, ZBS,**  
14 **YS and AM; Wrote the paper, PEF, MN, AP, ZBS, YS and AM.**

15 **4. Corresponding Author: Dr. Patrice E Fort**  
16 Associate Professor,  
17 Department of Ophthalmology & Visual Sciences, and Department of Molecular and  
18 Integrative Physiology, The University of Michigan, Ann Arbor, Michigan [Email-](mailto:patricef@umich.edu)  
19 [patricef@umich.edu](mailto:patricef@umich.edu)  
20

21 **5. Number of Figures: 7**

22 **6. Number of Tables: 1**

23 **7. Number of Multimedia: 0**

24 **8. Abstract-229**

25 **9. Significance statement - 120**

26 **10. Introduction- 891**

27 **11. Discussion- 1380**

28 **12. Acknowledgement: This research was performed in part supported by Research to**  
29 **Prevent Blindness (RPB).**

30 **13. Conflicts of Interest: Dr. Fort has intellectual property interests and is listed as inventor**  
31 **on a patent for the use of CryAA as a retinal neuroprotective treatment. The other**  
32 **authors declare no conflict of interest.**

33 **14. This research was supported by National Eye Institute (EY020895), NIH P30EY007003**  
34 **(Core Grant for Vision Research at the University of Michigan), and NIH P30DK020572**  
35 **(Michigan Diabetes Research Center) as well as the Lichter Award.**

36  
37

38

39

40 **Evidence for Paracrine Protective Role of Exogenous  $\alpha$ A-Crystallin in Retinal**  
41 **Ganglion Cells**

42

43

44 **Keywords:**  $\alpha$ A-Crystallins; Recombinant Proteins; Chaperone; Neuroprotection; Metabolic  
45 Stress

46

47 **Abstract:**

48 Expression and secretion of neurotrophic factors have long been known as a key mechanism of  
49 neuroglial interaction in the central nervous system. In addition, several other intrinsic  
50 neuroprotective pathways have been described, including those involving small heat shock  
51 proteins such as  $\alpha$ -crystallins. While initially considered as a purely intracellular mechanism,  
52 both  $\alpha$ A- and  $\alpha$ B-crystallins have been recently reported to be secreted by glial cells. While an  
53 anti-apoptotic effect of such secreted  $\alpha$ A-crystallin has been suggested, its regulation and  
54 protective potential remain unclear. We recently identified residue T148 and its phosphorylation  
55 as a critical regulator of  $\alpha$ A-crystallin intrinsic neuroprotective function. In the current study, we  
56 explored how mutation of this residue affected  $\alpha$ A-crystallin chaperone function, secretion, and  
57 paracrine protective function using primary glial and neuronal cells. After demonstrating the  
58 paracrine protective effect of  $\alpha$ A-crystallins secreted by primary Müller glial cells, we purified  
59 and characterized recombinant  $\alpha$ A-crystallin proteins mutated on the T148 regulatory residue.  
60 Characterization of the biochemical properties of these mutants revealed an increased  
61 chaperone activity of the phosphomimetic T148D mutant. Consistent with this observation, we  
62 also show that exogenous supplementation of the phosphomimetic T148D mutant protein  
63 protected primary retinal neurons from metabolic stress despite similar cellular uptake. In  
64 contrast, the non-phosphorylatable mutant was completely ineffective.

65 Altogether, our study demonstrates the paracrine role of  $\alpha$ A-crystallin in the central nervous  
66 system as well as the therapeutic potential of functionally enhanced  $\alpha$ A-crystallin recombinant  
67 proteins to prevent metabolic-stress induced neurodegeneration.

68

69 **Significance statement**

70  $\alpha$ A-crystallin is a chaperone protein that has been long known for its critical role in the lens  
71 proteostasis. Recent studies have highlighted the protective potential of  $\alpha$ A-crystallin in the  
72 central nervous system, especially the retina. The broad chaperone and cytoprotective functions  
73 of  $\alpha$ A-crystallin make it a very attractive target in the context of the dire need for novel protective  
74 therapies for neurodegenerative diseases. Our previous work has shown that phosphorylation  
75 on threonine 148 (T148) is a critical regulator of the cytoprotective function of  $\alpha$ A-crystallin. The  
76 current study demonstrates that  $\alpha$ A-crystallin secreted by Müller glial cells plays a paracrine  
77 protective role for retinal neurons. We further demonstrated the therapeutic potential of a  
78 functionally enhanced  $\alpha$ A-crystallin recombinant protein in promoting neuronal survival.

79

## 80 Introduction

81  $\alpha$ -Crystallins ( $\alpha$ A- and  $\alpha$ B-) have been extensively described as resident chaperone proteins in  
82 the eye lens and are imperative for maintaining transparency (Ghosh and Chauhan, 2019;  
83 Hejtmancik et al., 2015; Makley et al., 2015; Masilamoni et al., 2005). In recent years, both  
84 proteins gained substantial interest in the context of retinal insults and neurodegenerative  
85 diseases (Munemasa et al., 2009; Piri et al., 2013; Wang et al., 2011; Ying et al., 2008; Zhu and  
86 Reiser, 2018). Although the presence of  $\alpha$ -crystallins was initially described and studied in the  
87 ocular lens, their expression is not limited to this tissue.  $\alpha$ B-crystallin is ubiquitously expressed  
88 or stress-induced in most tissues and cells, including heart, skeletal muscle, kidney, lung, brain,  
89 and retina.  $\alpha$ A-crystallin, however, is basally expressed at low levels in a limited number of  
90 tissues while highly induced under stress conditions in the kidney and the central nervous  
91 system, including the retina (Dubin et al., 1991; Zhang et al., 2019). In the retina, both  $\alpha$ -  
92 crystallin proteins have been found predominantly in glia and retinal ganglion cells (RGCs) in  
93 the inner retina, as well as photoreceptors and retinal pigmental epithelium (RPE) in the outer  
94 retina (Kannan et al., 2016; Kase et al., 2012; Munemasa *et al.*, 2009; Rao et al., 2008;  
95 Ruebsam et al., 2018; Shi et al., 2015). Initially thought to be products of gene duplication, both  
96  $\alpha$ A- and  $\alpha$ B-crystallins are now known to present different expression patterns and functional  
97 roles, independent from each other, including in neuroprotection (Robinson and Overbeek,  
98 1996).

99 The neuroprotective function has been recently linked to both  $\alpha$ A- and  $\alpha$ B-crystallins in the  
100 context of different neurodegenerative diseases (Kannan *et al.*, 2016; Zhu and Reiser, 2018).  
101 Proposed mechanisms for these neuroprotective functions of  $\alpha$ -crystallin proteins include  
102 attenuation of mitochondrial dysfunction (Zhu and Reiser, 2018), reduced accumulation of  
103 misfolded proteins (Schmidt et al., 2012) and specific disruption of neuronal apoptotic pathways  
104 (Hua Wang et al., 2020; Piri *et al.*, 2013; Piri et al., 2016). Additionally, studies have established

105 a strong relationship between these two protein's expression and chaperone activity and their  
106 observed anti-apoptotic function (Pasupuleti et al., 2010; Piri *et al.*, 2013). As members of the  
107 small heat shock protein family,  $\alpha$ -crystallins have been shown to prevent protein aggregation  
108 as well as promote cell survival under conditions such as chemically induced hypoxia (Schmidt  
109 *et al.*, 2012; Yaung et al., 2008) including through inhibition of apoptosis. Expression of  $\alpha$ A- and  
110  $\alpha$ B-crystallins have been shown to increase in an experimental model of light-induced damage  
111 to the retina (Heinig et al., 2020), as well as at different stages of the wound healing process  
112 following retinal tear (Baba et al., 2015). Consistent with a protective potential for retinal  
113 neurons,  $\alpha$ -crystallin expression was also shown to correlate with increased RGC survival  
114 following optic nerve axotomy (Munemasa *et al.*, 2009) and in rescuing photoreceptors in a  
115 light-induced damage model (Heinig *et al.*, 2020).

116 Studies from our lab and others have reported an increased  $\alpha$ A-crystallin expression in the  
117 retinas of diabetic rodents as well as human donors with diabetes (Fort et al., 2009; Ruebsam *et*  
118 *al.*, 2018). However,  $\alpha$ A-crystallin function seemed to be impaired in the diabetic retina, as  
119 suggested by loss of solubility, and change in their post-translational modification (PTM) pattern  
120 (Reddy et al., 2013). PTMs have been reported to not only influence the structure but also the  
121 neuroprotective and chaperone functions of  $\alpha$ -crystallins (Heise et al., 2013; Kim et al., 2007).  
122 Specifically, phosphorylation on serine residues 19, 45, and 59 of  $\alpha$ B-crystallin (Heise *et al.*,  
123 2013; Kim *et al.*, 2007; Reddy *et al.*, 2013) and residue 122 and 148 of  $\alpha$ A-crystallin seem to be  
124 critical regulators of their chaperone and protective functions (Ruebsam *et al.*, 2018).  
125 Interestingly, while previous studies have shown increased phosphorylation for  $\alpha$ B-crystallin  
126 (Heise *et al.*, 2013; Reddy *et al.*, 2013),  $\alpha$ A-crystallin phosphorylation on residue 148 was  
127 dramatically reduced in the retina from diabetic rodents and diabetic donors, especially those  
128 with retinopathy (Ruebsam *et al.*, 2018). We also showed that the T148D phosphomimetic form  
129 of  $\alpha$ A-crystallin is a potent neuroprotector for retinal neurons against serum deprivation-induced



130 cell death (Ruebsam *et al.*, 2018). Furthermore, we have demonstrated that glial cells  
131 overexpressing  $\alpha$ A-crystallin secrete the protein in their extracellular environment and that  
132 supplementation of conditioned media from these cells efficiently promotes R28 cell survival  
133 following exposure to serum starvation-induced apoptotic stress (Ruebsam *et al.*, 2018).  
134 Interestingly, these observed anti-apoptotic effects were only observed from cells expressing  
135 the wild-type or phosphomimetic (T148D) protein, but not its non-phosphorylatable counterpart  
136 (T148A). While this pointed to a critical role of this phosphorylation, the impact of this post-  
137 translational modification on the structure-function relationship of  $\alpha$ A-crystallin remains  
138 unknown.

139 In all, our current understanding of  $\alpha$ -crystallin function draws out two major observations that 1)  
140  $\alpha$ A-crystallin serves a key neuroprotective function within the retinal tissue and 2)  
141 controlling/enhancing  $\alpha$ A-crystallin function presents the high potential to promote retinal cell  
142 survival and maintenance of the microarchitecture of the neuroretina. Therefore, in the present  
143 study, we studied the impact of T148D mutation of  $\alpha$ A-crystallin on its chaperone function and  
144 associated alteration of its biochemical properties. Furthermore, we assessed the potential of  
145 supplementation with recombinant T148D  $\alpha$ A-crystallin protein to promote survival of retinal  
146 neurons, especially primary RGCs, following exposure to metabolic stress. The current study,  
147 therefore, unveils an exciting new avenue for the use of  $\alpha$ A-crystallin and its functionally  
148 enhanced derivatives to slow the progression of retinal neurodegenerative disorders.

149

## 150 **Methods**

151 **Cell lines.** Rat retinal Müller cells (rMC-1) and retinal neuronal cell (R28) lines were obtained  
152 from Applied Biological Materials Inc. (Richmond, BC, Canada). All cell lines were maintained in  
153 DMEM, 5 mM Glucose (DMEM-NG) supplemented with 10 % FBS (Flow Laboratories) at 37 °C,

154 5 % CO<sub>2</sub> unless stated otherwise. For experiments, R28 cells were differentiated into neurons in  
155 DMEM with 8-(4-Chlorophenylthio) adenosine 3',5'-cyclic monophosphate (8-CPT-cAMP,  
156 Catalogue # C3912, Millipore Sigma, St. Louis, MO) at a final concentration of 2.5 mM on  
157 laminin-coated plates as described earlier (Ruebsam *et al.*, 2018).

158 **Primary Müller glial cells (MGCs)** were obtained from the  $\alpha$ A-crystallin knockout mice  
159 originally generously provided by Dr. Wawrousek from the National Eye Institute (NEI). Cells  
160 were isolated using a protocol adapted from Hicks and Courtois (Hicks and Courtois, 1990) and  
161 characterized previously (Brady *et al.*, 1997). Briefly, primary MGCs were isolated from the  
162 retinal tissue of P10-14  $\alpha$ A-crystallin knockout mice pups and maintained in DMEM-NG + 10%  
163 FBS + 1% Penicillin/Streptomycin (Catalogue # 15140122, Thermo Fisher Scientific, Waltham,  
164 MA). The purity and specificity of the cell preparation were validated by evaluating the  
165 expression of the Müller cell-specific markers glutamine synthetase, Prdx-6, and Abc8a from  
166 Passage 2-6 as described previously (Nath *et al.*, 2021).

167 **Primary retinal ganglion cells (RGCs).** RGCs were isolated and purified from  $\alpha$ A-crystallin  
168 knockout mice pups at P3-P5 using a modified immunopanning method described previously  
169 (Winzeler and Wang, 2013). The purified RGCs were resuspended in growth media containing  
170 B27 supplement (Thermo Fisher), 50 ng/ml BDNF (Catalogue # B3795, Millipore Sigma, St.  
171 Louis, MO), 10 ng/ml CNTF (Catalogue # C3835, Millipore Sigma, St. Louis, MO) and 4  $\mu$ g/ml  
172 forskolin (Catalogue # F3917, Millipore Sigma, St. Louis, MO) before being seeded onto poly-D-  
173 lysine and laminin-coated glass coverslips in 24-well culture plates. Cells were seeded at a  
174 density of 30,000 cells/cm<sup>2</sup> and the growth media was changed every three days until use.

175 ***Transient transfection of rMC-1 and MGCs and recovery of conditioned media.*** Cells were  
176 transfected using the Neon Transfection System (Invitrogen) following the manufacturer's  
177 instructions. Briefly, cells were trypsinized and washed in PBS before being resuspended in 110  
178  $\mu$ l resuspension buffer and electroporated with 2.5  $\mu$ g of the previously characterized pcDNA

179 3.1 vectors expressing either WT, the phosphomimetic T148D, or the non-phosphorylatable  
180 T148A crystallins, respectively (Ruebsam *et al.*, 2018) and were seeded in 6-well plates. The  
181 next day, transfected cells were incubated either in serum-free DMEM-NG (with 20mM  
182 Mannitol), DMEM-HG (DMEM-NG with 20 mM glucose), or DMEM-HG with 100ng/ml TNF $\alpha$   
183 (Catalogue # 210-TA, R&D systems, Minneapolis, MN) for 24 hours. Cells incubated in DMEM-  
184 NG served as the experimental control.

185 Following incubation, growth media from transfected glial cells was recovered and prepared as  
186 previously described (Ruebsam *et al.*, 2018). Briefly, the media was first filtered using a 0.22  $\mu$ m  
187 syringe filter (Catalogue #, Millipore Sigma, St. Louis, MO) and then centrifuged sequentially at  
188 300  $\times$  g for 6 minutes, 3,000  $\times$  g for 20 minutes, and 5,000  $\times$  g for 10 minutes at room  
189 temperature. Finally, the media were concentrated using 3K MWCO concentrators (Catalogue #  
190 C775, Amicon, Merck Millipore, USA) and stored at 4  $^{\circ}$ C until use in conditioned media  
191 experiments.

192 **Generation of recombinant  $\alpha$ A-crystallins.** pET23d+ vectors containing the cDNA sequence  
193 for human  $\alpha$ A-crystallin were used as a template for generating mutant proteins. Point mutations  
194 on T148 corresponding to the phosphomimetic (T148D) and the non-phosphorylatable (T148A)  
195 analogue of  $\alpha$ A-crystallin were introduced using the Quikchange Site-directed mutagenesis kit  
196 (Agilent Technologies, Santa Clara, CA) using primers listed in table 1. Cloned plasmids were  
197 scaled up in XL-1 Blue supercompetent cells, and isolated plasmid sequences were confirmed  
198 by Sanger sequencing. Sequenced plasmids were then used to transform BL21(DE3) pLysS  
199 cells to optimize the respective proteins' expression.

200 Cells were grown in LB Miller broth (Catalogue # BP142610P1, Fisher Scientific) in a rotary  
201 shaker maintained at 37  $^{\circ}$ C, 225 rpm, till they reached an OD<sub>600</sub> between 0.4-0.6. Protein  
202 expression was induced by the addition of isopropyl- $\beta$ -D-thiogalactopyranoside (IPTG,  
203 Catalogue # I2481C, GoldBio, St. Louis, MO) at a final concentration of 500  $\mu$ M for 4 hours.

204 Bacterial cell pellets were harvested by centrifugation at 4000 rpm for 20 minutes at 4 °C and  
205 stored overnight at - 80 °C. Cell Lysis and protein purification was carried out using size  
206 exclusion chromatography as described in (Horwitz et al., 1999). Purified proteins were  
207 subjected to endotoxin removal using Triton X-114 mediated phase separation using a protocol  
208 adapted from (Teodorowicz et al., 2017). The efficacy of endotoxin removal was ascertained  
209 using the Pierce™ Chromogenic Endotoxin Quant Kit (Catalogue # A39552, Thermo Fisher  
210 Scientific, Waltham, MA) as per manufacturer's instructions. Protein purity was assessed by  
211 Coomassie blue staining and Immunoblot analysis (Figure 3A). All proteins were stored in PBS  
212 pH 7.4 at - 80 °C until use.

213 **Chaperone activity assay.** The functional efficacy of purified  $\alpha$ A-crystallins to prevent non-  
214 specific protein aggregation *in vitro* was assessed by chaperone assays as described previously  
215 (Horwitz, 1992). Aggregation of 75  $\mu$ g alcohol dehydrogenase (ADH) in PBS pH 7.4 against  
216 varied amounts of  $\alpha$ A-crystallin was chemically induced by adding EDTA at a concentration of  
217 37.5 mM. Protein aggregation was monitored as relative absorbance at 360 nm in a FLUOstar  
218 OMEGA plate reader (BMG Labtech). Representative assays are an average of three  
219 independent experiments for statistical significance.

220 **Native gel electrophoresis.** The polydispersity profile of purified  $\alpha$ A-crystallins *in vitro* was  
221 assessed by Native PAGE gels. Samples were prepared using 7.5  $\mu$ g of recombinant WT,  
222 T148D or T148A  $\alpha$ A-crystallin resuspended in Novex™ Tris-Glycine Native Sample Buffer (2X)  
223 (Catalogue # [LC2673](#), Thermo Fisher Scientific) and deionized water. Samples were loaded on  
224 NativePAGE™ 3 to 12%, Bis-Tris gels (Catalogue # [BN1001BOX](#), Thermo Fisher Scientific).  
225 Gels were run using 1X NativePAGE™ Anode Buffer and 1X NativePAGE™ Dark Blue Cathode  
226 Buffer as per manufacturer's instructions. Gels were fixed and de-stained as per manufacturer's  
227 instructions and then imaged using a FluorChem™ E system (Protein Simple). Images were  
228 analyzed using the Gel Analyzer function of ImageJ (Schneider et al., 2012) and the molecular

229 size markers run on either side of the recombinant proteins, allowing us to obtain the median  
230 size of the oligomers for each recombinant protein. The area under the curve is shown as a  
231 function of oligomer sizes from less than 480 to 1236 kDa, with the median shown for each  
232 recombinant protein.

233 **Solubility assays.** As above, cells were transfected with 2.5  $\mu$ g of pcDNA 3.1(+) plasmids  
234 expressing either WT, T148D, or T148A crystallins or an empty vector (EV) and were seeded in  
235 6-well plates. The next day, transfected cells were incubated either in DMEM-NG + 10% FBS or  
236 serum-free DMEM-NG for 4 or 24 hours. Cells transfected with EV served as an experimental  
237 control. Following incubation, cells were harvested on ice in chilled RIPA buffer (100mM Tris pH  
238 7.5, 3mM EGTA, 5mM MgCl<sub>2</sub>, 0.5% Triton X-100, 1mM PMSF, 1X complete EDTA-free  
239 protease inhibitor cocktail tablet (Roche Diagnostics, Indianapolis, IN)) and subjected to  
240 immunoblot analyses.

241 **Protein uptake assay.** Differentiated R28 cells were allowed to grow on laminin-coated plates  
242 for 36 hours. Recombinant WT, T148D, or T148A crystallins were supplemented to growth  
243 media at a concentration of 500 ng/ml. Protein uptake in R28 cells was tested in DMEM-NG  
244 versus serum-free DMEM-NG, the presence and absence of BSA for 4 hours. Protein uptake by  
245 R28 cells was also tested under stress by incubating cells in serum-free DMEM-NG (with 20mM  
246 Mannitol), DMEM-HG (DMEM-NG with 20 mM glucose), or DMEM-HG with 100ng/ml TNF $\alpha$ .  
247 Following incubation, cells were harvested on ice in chilled RIPA buffer and subjected to  
248 immunoblot analyses.

249 **Proteinase K susceptibility assay.** Differentiated R28 cells were allowed to grow on laminin-  
250 coated 6-well plates for 36 hours. Recombinant WT  $\alpha$ A-crystallin was supplemented with growth  
251 media at a 500 ng/ml concentration for 2, 4, and 24 hours. The cell lysates were then subjected  
252 to proteinase K treatment as adopted by Ruebsam et al.,2018. Briefly, cell lysates were treated  
253 with 100 ng proteinase K (Millipore Sigma) in a reaction containing 10 mM Tris-HCl (pH 7.4)

254 with or without Triton X-100 (1%) for 30 minutes at 37°C. The reaction was stopped by the  
255 addition of loading buffer and heated at 70°C for 10 minutes. A control sample was treated the  
256 same way, aside from the omission of the enzymes. Protein levels were then assessed by  
257 immunoblotting as described below.

258

259 **Immunoblotting Analyses.** Protein concentrations were measured with the Pierce BCA  
260 reagent, and all samples and conditioned media were adjusted for equal protein concentration.  
261 To assess the purity of the recombinant protein preparations, 50 ng of pure protein was  
262 subjected to immunoblot analyses. For protein uptake experiments, cells were homogenized by  
263 sonication in RIPA buffer as described previously (Ruebsam *et al.*, 2018) and 35 µg of the total  
264 cell lysate was loaded on 4-12% NuPage Bis-Tris gels (Thermo Fisher). Gels were run in MES  
265 buffer (Thermo Fisher Scientific) as per manufacturer's instructions. Western blot transfer was  
266 carried out on nitrocellulose membranes using the Mini Trans-Blot cell (Catalogue # 1703930,  
267 Bio-Rad) at 160 V for 1 hour at 4 °C. For solubility assays, RIPA-soluble protein lysates were  
268 collected, and insoluble pellets were resuspended after PBS wash by sonication in Urea buffer  
269 (10mM Tris pH 7.5, 150mM NaCl, 5mM EGTA, 5mM MgCl<sub>2</sub>, 1mM DTT, 0.1% Triton X-100,  
270 0.2mM PMSF, 9M Urea). Soluble samples were adjusted for equal protein concentration, while  
271 insoluble samples were adjusted for equal volume. Samples were loaded on 4-12% NuPage  
272 Bis-Tris gels and run in MES buffer as per manufacturer's instructions, at 110 V. Cell lysates  
273 and conditioned media were immunoblotted for αA-crystallin (sc-28306, Santacruz  
274 Biotechnology, Dallas, TX) and β-actin (MAB-1501, Millipore) as a loading control. Solubility was  
275 measured as a ratio of insoluble αA-crystallin to total αA-crystallin for each condition (using the  
276 Gel Analyzer function in ImageJ (Schneider *et al.*, 2012), normalized to WT, and data were  
277 analyzed using the GraphPad Prism software module (GraphPad Software, San Diego, CA).

278 **Cell death Assay.** Cell death rates were assessed by DNA Fragmentation ELISA or TUNEL  
279 staining. For the DNA fragmentation ELISA (Roche Diagnostics, Indianapolis, IN), R28 cells  
280 were seeded in a 96 well plate at a density of  $1 \times 10^5$  cells per well and incubated with 100  $\mu$ l of  
281 conditioned medium for 4 hours before being processed according to the manufacturer's  
282 instructions and as previously described (Ruebsam *et al.*, 2018). The colorimetric signal was  
283 measured with a fluorescence plate reader in a FLUOstar OMEGA plate reader (BMG Labtech)  
284 with excitation at 405 and 490 nm.

285 For TUNEL staining, cells were seeded on glass coverslips as previously described. Following  
286 incubation, the coverslips were fixed in 4% PFA and stained for TUNEL (DeadEnd™  
287 Fluorometric TUNEL System, Promega) according to manufacturer's instructions. Briefly, the  
288 samples were incubated with fluorescent-labeled dUTP and TdT enzymes. The nuclei were  
289 visualized by Hoechst staining. Images were captured on a Leica DM6000 fluorescent  
290 microscope. Nuclei and TUNEL positive cells were counted using ImageJ (Schneider *et al.*,  
291 2012) and data were analyzed using the GraphPad Prism software module (GraphPad  
292 Software, San Diego, CA).

293 For primary RGC, characterization of the primary cells was performed by immunostaining with  
294 RGC specific markers –  $\beta$ 3-tubulin (Biolegend, Catalogue #801201), Neurofilament-H (NF-H,  
295 Millipore, Catalogue #NE1023), and RNA-binding protein with multiple splicing (RBPMS,  
296 (Rodriguez *et al.*, 2014), Genetex, Catalogue #GTX118169). For cell survival experiments, the  
297 coverslips were first subjected to TUNEL staining as described above. After TUNEL, the  
298 coverslips were immunostained with RBPMS antibody and secondary Alexa Flour 594 labeled  
299 antibody (Invitrogen, A21207). All Immunostainings were visualized, and images were captured  
300 using Leica DM6000 fluorescent microscope. Cells staining positive for RBPMS and both  
301 TUNEL and RBPMS were counted using the Imaris software module (Bitplane AG, Zurich,

302 Switzerland). The data were analyzed using GraphPad Prism (GraphPad Software, San Diego,  
303 CA).

304 **Statistics:**

305 For immunoblot experiments, the data were normalized to the housekeeping signal as a control  
306 before analysis. ANOVA models with heterogeneous variances, adjusted for the replication of  
307 the experiment, were fit to the data to assess differences between test and control group.  
308 Analyses were performed using nonrepeated-measures ANOVA, followed by the Tukey post-  
309 hoc tests for multiple comparisons, whereas 2-tailed t test was used for a single comparison.  
310 A P value less than 0.05 was considered significant.

311

312 **Results:**

313 **Expression and secretion of  $\alpha$ A-crystallin in MGCs.** Müller glial cells (MGCs) are  
314 instrumental in maintaining neuronal homeostasis in the retina, with defined functions ranging  
315 from the recycling of neurotransmitters to controlling ionic and water equilibrium (Dulle and Fort,  
316 2016). Our previous work emphasized the upregulation of  $\alpha$ A-crystallin in the glia and ganglion  
317 cell layers of retinal tissue from human donors with diabetes compared to non-diabetic controls.  
318 Furthermore, growth media from rMC-1 cells overexpressing  $\alpha$ A-crystallin efficiently promoted  
319 survival of R28 cells under serum starvation-induced apoptotic stress (Ruebsam *et al.*, 2018).  
320 To further investigate the role of  $\alpha$ A-crystallin in MGCs, we compared the relative expression of  
321  $\alpha$ A-crystallin in rMC-1 and primary Müller glial cells isolated from  $\alpha$ A-crystallin knockout mice.  
322 Cells from  $\alpha$ A-crystallin knockout mice were used throughout this study to avoid potential  
323 confounding effect of endogenously expressed and induced WT  $\alpha$ A-crystallin. Thus, cells  
324 lacking endogenous  $\alpha$ A-crystallin expression were transfected with either empty vectors or  
325 vectors driving expression of the wild-type protein (WT), the functionally enhanced



326 phosphomimetic (T148D), or the non-phosphorylatable (T148A) analogue, and  $\alpha$ A-crystallin  
327 expression was verified by immunoblot.

328 As we previously reported, WT, 148A, and 148D  $\alpha$ A-crystallin expressed well in transfected  
329 rMC-1. We also observed corresponding levels of secreted proteins in the cell culture media  
330 (conditioned media, **Figure 1A, left panel**). Additionally, the expression of all three crystallin  
331 constructs was consistent in the cell lysate and conditioned media under normal conditions as  
332 well as under conditions of metabolic and "diabetes-like" stress (**Figure 1A, middle and right**  
333 **panel**). Importantly, we also report that primary MGCs could be transfected with the same  
334 vectors, leading to expression levels and secretion comparable to those seen in rMC-1 (**Figure**  
335 **1B**). Similar to rMC-1, our data also clearly show that stress exposure does not affect the  
336 expression and secretion of any of our  $\alpha$ A-crystallin constructs.

337 **Neuroprotective potential of MGC secreted  $\alpha$ A-crystallin.** Overexpression of  $\alpha$ A-crystallin in  
338 multiple cell models has demonstrated its anti-apoptotic potential under conditions of stress-  
339 induced cell death (Christopher et al., 2014; Liu et al., 2004; Losiewicz and Fort, 2011;  
340 Pasupuleti et al., 2010; Ruebsam et al., 2018). To investigate the protective potential of MGC  
341 secreted  $\alpha$ A-crystallin, we tested the effect of conditioned media obtained from  $\alpha$ A-crystallin  
342 transfected primary MGCs on retinal neurons subjected to metabolic stress. Supplementation of  
343 conditioned media from MGCs overexpressing WT and T148D crystallin highly promoted R28  
344 cell survival under serum starvation-induced metabolic stress, as evidenced by the reduction in  
345 cell death by 45% and 37%, respectively. Similarly, in "diabetes-like" stress, conditioned media  
346 from MGCs overexpressing WT or 148D  $\alpha$ A-crystallin resulted in 38% and 44% reduction in  
347 R28 cell death, respectively. Supportive of the key role of T148 phosphorylation, media from  
348 T148A overexpressing MGCs was ineffective in promoting R-28 cell survival in either stress  
349 (**Figure 2A and B**). Immunoblot analysis of the cell lysate and conditioned media confirmed that  
350 this difference in protective effect was not due to lower levels of expression or secretion of

351 T148A (**Figures 2C and D**). We then tested the effect of conditioned media on primary,  $\alpha$ A-  
352 crystallin knockout (AKO) mouse RGCs. As in R28 cells, supplementation of conditioned media  
353 from MGCs overexpressing WT and T148D crystallin highly promoted RGC survival under  
354 "diabetes-like" stress, while media from T148A overexpressing MGCs did not (**Figure 2E**).  
355 Taken together, these data clearly demonstrate the neuroprotective potential of  $\alpha$ A-crystallin  
356 and validate a paracrine role of MGC secreted  $\alpha$ A-crystallin in promoting neuronal cell survival  
357 under stress.

358 **Characterization of recombinant  $\alpha$ A-crystallins.** Our experiments with secreted  $\alpha$ A-crystallin  
359 highlighted the neuroprotective potential of extracellular WT and T148D crystallins in promoting  
360 neuronal cell survival exposed to serum starvation and "diabetes-like" conditions. This prompted  
361 us to assess if our observation from the conditioned media experiments could be recapitulated  
362 using purified, recombinant  $\alpha$ A-crystallin proteins. All three proteins, WT, T148A, and T148D  
363 were scaled up from BL21(DE3) pLysS cells expressing the specified constructs and purified by  
364 size exclusion chromatography. As shown in **Figure 3A**, the three purified proteins show a high  
365 degree of purity, as validated by SDS-PAGE and immunoblotting analyses. Because  
366 recombinant proteins purified from bacterial sources are often contaminated with bacterial  
367 endotoxins, which compromises their use *in vivo*, our protein preparations were treated with  
368 Triton X-114, a treatment routinely used to promote efficient endotoxin removal (Teodorowicz *et*  
369 *al.*, 2017). Qualitative analysis of the recombinant protein preparations post Triton X-114  
370 mediated phase separation confirmed the more than 90% reduction in the total endotoxin  
371 content (**Figure 3B**).

372  $\alpha$ A-crystallins were initially characterized in the eye lens as chaperone proteins, efficiently  
373 preventing non-specific protein aggregation and promoting organ transparency. *In vitro*, we  
374 tested the relative chaperone function of WT, T148D, and T148A crystallins by employing  
375 aggregation kinetics assays. As previously shown, EDTA-induced aggregation of ADH was

376 suppressed by  $\alpha$ A-crystallins in a concentration-dependent manner (**Figure 3C**). Consistent with  
377 enhancing  $\alpha$ A-crystallin chaperone activity by its phosphorylation on T148, the T148D mutant  
378 was significantly more effective at preventing ADH aggregation *in vitro* (**Figure 3D**). While the  
379 WT  $\alpha$ A-crystallin exhibited an IC<sub>50</sub> of 8  $\mu$ g, that of the T148D crystallin mutant was 4.4  $\mu$ g,  
380 demonstrating an increase in chaperone efficacy of 45 percent. The phosphorylation of  $\alpha$ A-  
381 crystallin on T148, therefore, results in an enhancement of its chaperone function.

382 **Stress-induced insolubility of  $\alpha$ A-crystallin.** WT, T148D, and T148A  $\alpha$ A-crystallin expressed  
383 in R28 cells exhibited no differences in basal solubility (**Figure 4A**). However, following 4 hours  
384 of serum starvation, T148A trended towards higher insolubility, and T148D trended toward lower  
385 insolubility (data not shown), an effect confirmed and enhanced after 24 hours of serum  
386 starvation (**Figure 4B**). This observation indicates that phosphorylation on residue T148 plays a  
387 key role in promoting  $\alpha$ A-crystallin's function, including by reducing stress-induced insolubility.

388 **T148 phosphorylation-dependent changes in oligomer size.**  $\alpha$ A-crystallin, along with its  
389 close relative  $\alpha$ B-crystallin is known to exist as larger oligomers, we thus assessed how this  
390 phosphorylation impacts the oligomeric state of  $\alpha$ A-crystallin. T148A  $\alpha$ A-crystallin formed  
391 slightly larger oligomers (median 669 kDa) than the WT  $\alpha$ A-crystallin (median 650 kDa),  
392 whereas T148D formed substantially smaller oligomers (median 613 kDa; Figure 4C-D). This  
393 data is clearly supportive of the T148 phosphorylation state impacting oligomeric and potentially  
394 aggregate formation. This could also partially explain the solubility data as the decreased  
395 oligomeric size observed for the T148D mutant could promote the protein's solubility under  
396 stress conditions. Together the solubility and oligomeric data are consistent with the relative  
397 pro-survival potential of the mutants. As  $\alpha$ A-crystallin becomes more insoluble and/or forms  
398 larger oligomers, less is likely available to serve normal chaperone and protective roles.

399 **Uptake of recombinant  $\alpha$ A-crystallins.** Our previous study showed that conditioned media  
400 from MGCs expressing  $\alpha$ A-crystallins WT and T148D greatly reduced stress-induced R28 cell  
401 death. Prior to testing the neuroprotective efficacy of the different recombinant  $\alpha$ A-crystallins, we  
402 first characterized the specificity of their uptake in R28 cells. As expected, supplementation of  
403 recombinant  $\alpha$ A-crystallins to differentiated R28 cells showed a gradual increase in their uptake  
404 as a function of time (**Figure 5A**). We then assessed the impact of stress on protein uptake and  
405 showed that serum starvation was associated with an increased uptake of all recombinant  
406 proteins, including T148A, although slightly less than WT and T148D  $\alpha$ A-crystallins. Since  
407 T148A is taken up by the cells under stress, it can be asserted that the level of protein uptake is  
408 not solely responsible for the relative protective efficacy of the different recombinant proteins.

409 To eliminate the possibility that the increased uptake of recombinant proteins observed in serum  
410 starvation is facilitated by the lack of interactions that would otherwise occur with components of  
411 FBS, we spiked the growth media with saturating concentrations of BSA (1%). Supplementation  
412 of BSA did not impact protein uptake, suggesting the difference in uptake of proteins as part of  
413 the stress response (**Figure 5B**). The level of protein uptake was further investigated by  
414 characterizing protein uptake under "diabetes-like" conditions (**Figure 5C**). Protein uptake  
415 progressively increased in cells exposed to "diabetes-like" conditions (HG, HG+TNF $\alpha$  lanes)  
416 and is independent of T148 mutation (**Figure 5C**). Collectively, our data demonstrate that T148  
417 mutation does not dramatically impact its uptake by R28 cells in a way that could significantly  
418 affect its observed neuroprotective efficacy under stress.

419 Following the uptake assay of recombinant proteins, the R28 cells were further assessed for the  
420 internalization of these proteins. The obtained results have demonstrated the time-dependent  
421 marked expression of recombinant WT  $\alpha$ A-crystallin in R-28 cells in the intact cell membrane  
422 during protease digestion. On the contrary, the intracellular access of protease in R-28 cells led

423 to the complete digestion of WT  $\alpha$ A-crystallin, confirming the internalization of  $\alpha$ A-crystallin  
424 recombinant proteins in cells upon its extracellular supplementation (**Figure 5D**).

425 **Effect of  $\alpha$ A-crystallin supplementation on neuronal cell viability.** To test the effect of  
426 uptake of recombinant  $\alpha$ A-crystallins on cell viability under conditions of stress, we sought to  
427 establish a dose-response effect of  $\alpha$ A-crystallin concentration on R28 cell viability. External  
428 supplementation of WT  $\alpha$ A-crystallin efficiently prevented serum starvation-induced R28 cell  
429 death in a dose-dependent manner (**Figure 6A**) as validated by TUNEL staining. Approximately  
430 60% reduction in R28 cell death was observed following incubation with 500 ng/ml WT  $\alpha$ A-  
431 crystallin, and this dose was selected to assess the relative neuroprotective efficacy of T148D  
432 and T148A crystallins in comparison to WT. Figure 5B summarizes the relative efficacies of 500  
433 ng/ml WT, T148D, and T148A crystallins in promoting R28 cell survival in response to serum  
434 starvation-induced apoptotic stress. Compared to control, incubation with 500 ng/ml T148D  
435 crystallin resulted in ~ 85% increased cell viability in comparison to WT (~ 30%). Incubation with  
436 500 ng/ml T148A did not promote R28 cell viability, further validating the key role of  
437 phosphorylation of  $\alpha$ A-crystallin on T148 for its neuroprotective function (**Figure 6B**).

438 To confirm the neuroprotective efficacy of recombinant  $\alpha$ A-crystallins in promoting neuronal cell  
439 survival, we further tested the ability of the recombinant protein supplementation on the survival  
440 of primary retinal ganglion cells (RGCs) under "diabetes-like" conditions. As to avoid potential  
441 complications due to induction of endogenous  $\alpha$ A-crystallin, RGCs were also isolated from the  
442 retinas of  $\alpha$ A-crystallin knockout mice, and the purity of the RGC preparation was assessed by  
443 staining for neuronal cell-specific markers (**Figures 7A-C**). RGCs cell death under "diabetes-  
444 like" conditions was then analyzed by TUNEL and RBPMS co-staining. Consistent with the  
445 effect seen in differentiated R28 cells, supplementation with 500 ng/ml of WT or T148D  $\alpha$ A-  
446 crystallins were highly protective of RGC cells exposed to metabolic stress (**Figure 7D & E**).  
447 Also similar to what was observed in R28 cells, co-incubation with T148D was slightly more

448 protective than WT while T148A crystallin completely failed to prevent cell death, emphasizing  
449 an inherent role of T148 phosphorylation on the neuroprotective efficacy of  $\alpha$ A-crystallin.

450

451 **Discussion:**

452 Our present study has shown that primary Müller glial cells can secrete  $\alpha$ A-crystallin and that  
453 secreted  $\alpha$ A-crystallin presents with significant neuroprotective abilities for retinal neuronal cells  
454 exposed to metabolic stresses. Supportive of a paracrine function of the secreted protein and  
455 therapeutic potential for  $\alpha$ A-crystallin recombinant proteins was the demonstration of its  
456 increased uptake in stressed retinal neurons. Furthermore, analysis of the biochemical and  
457 biophysical properties of these recombinant proteins revealed an increased chaperone activity,  
458 smaller oligomer assembly, and an increased solubility of the T148D  $\alpha$ A-phosphomimetic,  
459 consistent with its enhanced protective effect. Overall, our study shows that supplemented  $\alpha$ A-  
460 crystallin recombinant proteins are neuroprotective for primary retinal neurons exposed to  
461 metabolic stress and that  $\alpha$ A-crystallin T148D phosphomimetic mutant presents with enhanced  
462 therapeutic ability.

463 Müller glia has been shown to release trophic factors which regulate the various aspects of  
464 retinal neuronal circuitry during the process of synaptogenesis, differentiation, neuroprotection,  
465 and survival of photoreceptors and RGCs in the retina (de Melo Reis et al., 2008). Müller glial  
466 cells, astrocytes, and microglia also play an important role in the metabolism, the phagocytosis  
467 of neuronal debris, the release of certain neurotransmitters, and the release of trophic factors  
468 apart from providing structural support (Vecino et al., 2016). They are also reported to be  
469 involved in the inflammation associated with the pathophysiology of diabetic retinopathy, with  
470 special emphasis on the functional relationships between glial cells and neurons (Rubsam et al.,  
471 2018). Müller glial cells are an important source of numerous pro-survival factors under

472 inflammatory conditions to exert neuroprotection, a potentially key point in patients with DR  
473 since they have higher levels of both inflammatory cytokines and neurotransmitters in their  
474 vitreous (Boss et al., 2017).

475 More recently, it also has been observed that non-toxin-induced Müller cell ablation is  
476 detrimental for neurons further supporting their necessity for neuronal viability (Fu et al., 2015).  
477 Stem cell-derived RGC-like cells survival was substantially enhanced when co-cultured with  
478 adult Müller cells or supplemented with Müller cell-conditioned media and significantly increased  
479 their neurite length (Pereiro et al., 2020). Confluent retinal Müller glial cell substrates and its  
480 conditioned medium were also reported to significantly increase the survival of cultured porcine  
481 RGCs (Garcia et al., 2002). Our current study has also demonstrated that retinal Müller glial  
482 cells were able to secrete  $\alpha$ A-crystallin, and incubation of either R28 retinal neuronal cells or  
483 primary  $\alpha$ A-crystallin knockout (AKO) mouse RGCs with the conditioned media resulted in a  
484 significant decrease in the cell death induced by metabolic stress. Our study further confirmed  
485 the importance of T148 phosphorylation in the neuroprotective function of  $\alpha$ A-crystallin as  
486 evidenced by the greater protection of retinal neurons by the phosphomimetic mutant  
487 conditioned media, while the non-phosphorylatable mutant conditioned media had no effect.

488 The effect of phosphorylation on the structure and function of  $\alpha$ -crystallin has largely been  
489 studied for  $\alpha$ B-crystallin, owing to its ubiquitous distribution and upregulation under stress and  
490 disease conditions. Studies investigating chaperone and anti-apoptotic activity of  
491 phosphorylated  $\alpha$ B-crystallin mostly support a pro-chaperone and anti-apoptotic enhancer role  
492 of this phosphorylation under various cellular stresses while underlying a more complex function  
493 during development and cancer (Morrison et al., 2003) (Jeong et al., 2012) (Lee et al., 2016). In  
494 the meantime, the effect of phosphorylation on the chaperone function and the anti-apoptotic  
495 activity of  $\alpha$ A-crystallin have evaded diligent investigation.

496 Takemoto et al. first reported an increase in the phosphorylation of  $\alpha$ A-crystallin on S122 from  
497 donor lens tissue in an age-dependent fashion (Takemoto, 1996). 2D gel electrophoresis on  
498 lens tissue of 14-week C57BL6 mice identified T148 in addition to S122 as sites of  
499 phosphorylation on  $\alpha$ A-crystallin (Reddy et al., 2006). A recent study from our lab was the first to  
500 identify T148 phosphorylation *in vivo* from retinal tissue samples from human donors (Ruebsam  
501 et al., 2018). The modification was dramatically reduced in donor samples with diabetes,  
502 suggesting an inherent role for T148 phosphorylation of  $\alpha$ A-crystallin in the pathophysiology of  
503 diabetic retinopathy (DR). Overexpression of the  $\alpha$ A-crystallin phosphomimetic T148D conferred  
504 protection to R28 neuronal cells to serum starvation-induced apoptosis over its non-  
505 phosphorylatable analog T148A. The current study, therefore, investigated the structural and  
506 functional consequences of T148 phosphorylation on  $\alpha$ A-crystallin.

507 Mutations in  $\alpha$ A-crystallin have been shown to influence its chaperone activity. Recombinant  
508  $\alpha$ A-T148D crystallin exhibited maximal efficiency in preventing EDTA-induced aggregation of  
509 Alcohol dehydrogenase over wild-type and T148A crystallin. In conjunction with the observed  
510 cytoprotective effect observed in the earlier study, it shows that phosphorylation of T148  
511 enhances the chaperone function and the associated anti-apoptotic function of retinal  $\alpha$ A-  
512 crystallin. Both  $\alpha$ -Crystallin proteins have been shown to associate into large oligomeric  
513 structures with molar masses ranging from 400-700 kDa. Our study has shown that  
514 phosphorylation of  $\alpha$ A-crystallin was directly influencing the oligomeric assembly of  $\alpha$ A-crystallin  
515 *in vitro*. Native gel analysis of recombinant  $\alpha$ A-crystallins suggests a change in the  
516 polydispersity profile of T148D crystallin, which showed an increased predisposition to form  
517 smaller oligomeric assemblies when compared to the wild type and T148A  $\alpha$ A-crystallin. Since  
518 the chaperone activity of  $\alpha$ -crystallin has been shown to be modulated by hydrophobic 'patches'  
519 distributed along with its monomeric structure (Datta and Rao, 1999; Rao et al., 1998). The  
520 observed oligomeric shift in our present study could translate into a higher number of smaller



521 oligomers exerting their chaperone action. Studies have also demonstrated that exposure of  
522 hydrophobic residues by structural modification facilitates chaperoning in  $\alpha$ -crystallin proteins  
523 whereas the flexible carboxy-terminal extension also contributes to the chaperone activity by  
524 enhancing the solubility (MacRae, 2000; Ruebsam *et al.*, 2018). The change in oligomeric  
525 profile was less pronounced for T148A crystallin, which was to be expected, as the recombinant  
526 WT crystallin protein used in this experiment was similarly unphosphorylated. However, this  
527 difference may become more pronounced in the cellular environment as WT  $\alpha$ A-crystallin  
528 becomes phosphorylated and explains the lack of protective ability of T148A recombinant  
529 proteins *in vitro*.

530  $\alpha$ A-crystallin was originally described as an endogenous neuroprotective factor in retinal  
531 neurons, as exhibited in over-expression-based studies in hypoxic stress, or glaucomatous and  
532 other optic neuropathies (MacRae, 2000). Several studies have also demonstrated that  $\alpha$ A-  
533 crystallin enhanced endogenous expression has potential as the therapeutic strategy to protect  
534 and rescue neurons from degeneration associated with metabolic or hypoxic stress (MacRae,  
535 2000; Ying *et al.*, 2014). Similarly, exogenous supplementation of  $\alpha$ A-crystallin via intravitreal  
536 injections was associated with significantly decreased levels of GFAP in both the retina and the  
537 crush site following the 3rd day of optic nerve crush injury and induced astrocytes architecture  
538 remodeling at the crush site (Piri *et al.*, 2016). In the increased intraocular pressure model,  
539 intravitreal injection of  $\alpha$ B-crystallin was also able to increase RGCs survival and function, as  
540 measured by functional photopic electroretinogram, retinal nerve fiber layer thickness, and RGC  
541 counts (Shao *et al.*, 2016). Another study has reported the enhanced rate of survival in the  
542 axotomized axons beyond the crush site after a single intravitreal administration of  $\alpha$ -crystallin  
543 at the time of axotomy (Anders *et al.*, 2017). Together with these previous reports, the present  
544 study strongly supports the protective potential of functionally enhanced  $\alpha$ A-crystallin  
545 recombinant proteins against neurodegeneration.

546 **Conclusion:**

547 In conclusion, our study demonstrates for the first time that the exogenous supplementation of  
548  $\alpha$ A-crystallin, especially its functionally enhanced mutant, promotes retinal cell survival under  
549 metabolic stress. Altogether, our data show that  $\alpha$ A-crystallin recombinant proteins present a  
550 strong potential to reduce neuronal cell death during acute stresses and that its T148D  
551 phosphomimetic mutant form could be an interesting option in chronic diseases such as  
552 diabetes, due to its improved biochemical properties and enhanced functionality. *In vivo* studies,  
553 including in diabetes models are now essential to further demonstrate the potential of this  
554 approach and validate the neuroprotective effect of functionally enhanced  $\alpha$ A-crystallin  
555 recombinant proteins. These studies will also be key in characterizing the mechanisms of action  
556 of  $\alpha$ A-crystallin *in vivo* in order to unveil  $\alpha$ A-crystallin specific involvement in the regulation of  
557 neurosurvival and neuroinflammation.

558 **Acknowledgment:** This research was supported by National Eye Institute (EY020895), NIH  
559 P30EY007003 (Core Grant for Vision Research at the University of Michigan), and NIH  
560 P30DK020572 (Michigan Diabetes Research Center) as well as the Lichter Award, Research to  
561 Prevent Blindness (RPB).

562 **Author Contributions:** Conceptualization, Patrice Fort; Data curation, Madhu Nath, Ashutosh  
563 Phadte, Zachary B. Sluzala, Yang Shan and Angela Myers; Formal analysis, Madhu Nath,  
564 Ashutosh Phadte, Zachary B. Sluzala, Yang Shan and Patrice Fort; Funding acquisition, Patrice  
565 Fort; Investigation, Madhu Nath, Zachary B. Sluzala, Ashutosh Phadte and Yang Shan;  
566 Methodology, Madhu Nath, Zachary B. Sluzala, Ashutosh Phadte and Yang Shan; Project  
567 administration, Patrice Fort; Resources, Angela Myers and Patrice Fort; Software, Madhu Nath,  
568 Zachary B. Sluzala, Ashutosh Phadte and Yang Shan; Supervision, Patrice Fort; Writing –  
569 original draft, Ashutosh Phadte, Madhu Nath, Zachary B. Sluzala and Patrice Fort; Writing –

570 review & editing, Ashutosh Phadte, Madhu Nath, Zachary B. Sluzala, Yang Shan, Angela Myers  
571 and Patrice Fort.

572 **Institutional Review Board Statement:** All experiments were conducted following the  
573 Association for Research in Vision and Ophthalmology Resolution on the Care and Use of  
574 Laboratory Animals and approved by the Institutional Animal Care and Use Committee of the  
575 University of Michigan (Protocol No: PRO-00009143 approved 7/9/2019).

576 **Informed Consent Statement:** Not applicable.

577 **Data Availability Statement:** Data generated is included within the manuscript.

578

#### 579 **Figure Legends**

580 **Figure 1. Expression and secretion of  $\alpha$ A-crystallins by Müller cells.**  $\alpha$ A-crystallin (CRYAA)  
581 expression was observed in the cell lysates and the concentrated growth (conditioned) media.  
582 **(A)** Rat retinal Müller (rMC-1) cells and **(B)** primary Müller cells isolated from  $\alpha$ A-crystallin  
583 knockout (KO) mice were transfected with either empty vector (EV), wild type  $\alpha$ A-crystallin (WT),  
584  $\alpha$ A-crystallin phosphomimetic (T148D), and the non-phosphorylatable form of  $\alpha$ A-crystallin  
585 (T148A). 24 hours post-transfection, cells were either exposed to normal media (DMEM-NG +  
586 10% FBS), serum starvation (DMEM-NG No FBS), or diabetic-like stress (DMEM-NG + 20 mM  
587 glucose +100ng/ml TNF $\alpha$ ) for 4 hours.

588 **Figure 2: MGC secreted  $\alpha$ A-crystallin promotes neuronal cell survival under stress.** The  
589 relative viability of rat retinal neuronal (R28) cells under **(A)** serum starvation stress and **(B)**  
590 “Diabetes-like” condition, following supplementation of ‘conditioned’ media from MGCs  
591 overexpressing  $\alpha$ A-crystallin. (\*P  $\leq$  0.05), (\*\*P  $\leq$  0.01), (\*\*P  $\leq$  0.001), significantly different from  
592 respective EV-transfected cells. Representative endpoint statistics result of DNA fragmentation  
593 ELISA from three replicates, with relative significance determined by 1-way ANOVA followed by  
594 the Tukey post-hoc tests test. Immunoblotting analyses reveal a similar expression pattern of  
595 WT, T148A, and T148D crystallins in comparison to EV control under **(C)** serum starvation  
596 stress and **(D)** “Diabetes-like” condition. **(E)** The relative viability of primary,  $\alpha$ A-crystallin  
597 knockout (AKO) mouse retinal ganglion cells (RGC) under basal and stress conditions following

598 supplementation of 'conditioned media' (CM) from MGCs overexpressing  $\alpha$ A-crystallin.  
599 Representative endpoint statistics result of TUNEL from 3-4 fields from three coverslips per  
600 condition of three replicates, with relative significance determined by 1-way ANOVA followed by  
601 Tukey post-hoc tests. The data was expressed as mean  $\pm$  SD and statistically significant  
602 differences are reported. (\*\*P  $\leq$  0.01), (\*\*P  $\leq$  0.001), (\*\*\*\*P  $\leq$  0.0001), significantly different from  
603 respective EV-transfected cells.

604 **Figure 3. Characterization of recombinant  $\alpha$ A-crystallins.** (A) BL21 purified  $\alpha$ A-crystallins  
605 were analyzed for purity using SDS page (top panel) and western blot (bottom panel),  
606 respectively. (B) Triton X-114 treatment of purified  $\alpha$ A-crystallins drastically reduces their  
607 relative endotoxin content in comparison to non-treated controls. 500 ng of each of the purified  
608 proteins was subjected to endotoxin estimation using the LAL assay kit. (C) Chaperone assays  
609 with ADH show a  $\alpha$ A-crystallin concentration-dependent decrease in ADH aggregation,  
610 monitored as relative absorbance at 360 nm. The range of  $\alpha$ A-crystallin concentrations used is  
611 depicted in the legend. (D) *In vitro* chaperone activity assays reveal an enhanced chaperone  
612 function of T148D crystallin over  $\alpha$ A-WT (n=3). The data are represented as mean  $\pm$  SD and  
613 statistically significant differences are reported. (\*\*P  $\leq$  0.01), (\*\*P  $\leq$  0.001), (\*\*\*\*P  $\leq$  0.0001),  
614 significantly different from respective EV-transfected cells.

615 **Figure 4. Phosphomimetic and non-phosphorylatable mutants of  $\alpha$ A-crystallin exhibit**  
616 **differences in stress-induced solubility and oligomeric profile.** (A) Representative blot  
617 showing relative amounts of soluble (S) and insoluble (I)  $\alpha$ A-crystallin after 24 hours of serum  
618 deprivation. (B) Solubility differences are expressed as a ratio of insoluble  $\alpha$ A-crystallin to total  
619  $\alpha$ A-crystallin for each condition, normalized to WT. Data are represented as mean  $\pm$  S.D.  
620 Statistical comparisons between groups were calculated by One-Way ANOVA followed by  
621 Tukey post-hoc tests (\*\*p<0.01). (C) Representative Native gel showing the oligomeric profiles  
622 of WT, T148D and T148A  $\alpha$ A-crystallin. (D). Graphical representation of oligomeric profiles of  
623 the native gels (representative of 3 independent experiments). Median oligomer size for each  
624 recombinant protein is shown, rounded to the nearest kilodalton.

625 **Figure 5. Selective uptake of recombinant  $\alpha$ A-crystallins by R28 cells.** All recombinant  
626 proteins were supplemented at a concentration of 500 ng/ml. (A) Time dependent uptake of  
627 recombinant  $\alpha$ A-crystallins by R28 cells under serum starvation induced metabolic stress.  
628 Uptake of  $\alpha$ A-crystallins in R28 cells was dependent on the presence of serum (B) and  
629 specificity of induced "diabetes-like" conditions (C) as mimicked by supplementation of DMEM-  
630 NG  $\pm$  10% FBS  $\pm$  1% BSA and DMEM-HG (25mM) + 10 % FBS  $\pm$  100 ng/ml TNF $\alpha$  respectively.

631 (D) Supplemented recombinant  $\alpha$ A-crystallins were internalized in the R28 cells as assessed by  
632 Proteinase K susceptibility assay.

633 **Figure 6. Effect of  $\alpha$ A-crystallin supplementation on R28 cell viability under stress.** All  
634 proteins were supplemented to R28 cells in DMEM-NG  $\pm$  10% FBS. Following treatment, cell  
635 viability was assessed by TUNEL staining. (A) Supplementation of WT suppresses serum  
636 starvation induced R28 cell death in a dose dependent manner. (B) T148D crystallin  
637 supplementation efficiently prevents R28 cell death under serum starvation induced metabolic  
638 stress compared to WT and T148A. Data are representative of four fields from three coverslips  
639 per condition and are represented as mean  $\pm$  S.D. from (\*\*\*:  $p \leq 0.0005$ ), (\*\*\*\*:  $p \leq 0.000005$ ),  
640 significantly different from respective EV.

641 **Figure 7. Exogenous  $\alpha$ A-crystallin protects primary mice retinal ganglion cells under**  
642 **stress.** (A) Seven days post seeding, the RGCs show prominent neural processes. (B)  
643 Immunofluorescence analyses highlight prominent staining for neuron-specific  $\beta$ III-tubulin (B,  
644 red), (C) neurofilament (NF-H, green), and RBPMS (red). (D) Vehicle control (VC), Recombinant  
645 wild type  $\alpha$ A-crystallin (WT),  $\alpha$ A-crystallin phosphomimetic (T148D), and the non-  
646 phosphorylatable form of  $\alpha$ A-crystallin (T148A) were supplemented to RGCs at a 500 ng/ml  
647 concentration and incubated for 8 hours with 25 mM D-glucose (HG) and 100 ng/ml TNF $\alpha$  for 8  
648 hours. Cells incubated with 5mM glucose (NG) served as an experimental control. RGC survival  
649 under stress was assessed by TUNEL staining (green), and cells were later stained for RBPMS  
650 (red). (E) Statistical analyses of RGC viability following exposure to stress. Percentage of  
651 apoptotic cells (TUNEL positive) in all RGCs (RBPMS positive) were analyzed. Data are  
652 represented as mean  $\pm$  S.D. Statistical comparisons between groups were calculated by One-  
653 Way ANOVA followed by Tukey post-hoc tests. (\*\*P  $\leq$  0.01), (\*\*P  $\leq$  0.001), (\*\*\*\*P  $\leq$  0.0001),  
654 significantly different from respective EV-transfected cells.

655

656

657 **References**

- 658 Anders, F., Liu, A., Mann, C., Teister, J., Lauzi, J., Thanos, S., Grus, F.H., Pfeiffer, N., and Prokosch, V.  
659 (2017). The Small Heat Shock Protein alpha-Crystallin B Shows Neuroprotective Properties in a  
660 Glaucoma Animal Model. *Int J Mol Sci* *18*. 10.3390/ijms18112418.
- 661 Baba, T., Oshitari, T., and Yamamoto, S. (2015). Level of vitreous alpha-B crystallin in eyes with  
662 rhegmatogenous retinal detachment. *Graefes Arch Clin Exp Ophthalmol* *253*, 1251-1254.  
663 10.1007/s00417-014-2815-z.
- 664 Boss, J.D., Singh, P.K., Pandya, H.K., Tosi, J., Kim, C., Tewari, A., Juzych, M.S., Abrams, G.W., and Kumar,  
665 A. (2017). Assessment of Neurotrophins and Inflammatory Mediators in Vitreous of Patients With  
666 Diabetic Retinopathy. *Invest Ophthalmol Vis Sci* *58*, 5594-5603. 10.1167/iovs.17-21973.
- 667 Brady, J.P., Garland, D., Duglas-Tabor, Y., Robison, W.G., Jr., Groome, A., and Wawrousek, E.F. (1997).  
668 Targeted disruption of the mouse alpha A-crystallin gene induces cataract and cytoplasmic inclusion  
669 bodies containing the small heat shock protein alpha B-crystallin. *Proc Natl Acad Sci U S A* *94*, 884-889.
- 670 Christopher, K.L., Pedler, M.G., Shieh, B., Ammar, D.A., Petrash, J.M., and Mueller, N.H. (2014). Alpha-  
671 crystallin-mediated protection of lens cells against heat and oxidative stress-induced cell death. *Biochim*  
672 *Biophys Acta* *1843*, 309-315. 10.1016/j.bbamcr.2013.11.010.
- 673 Datta, S.A., and Rao, C.M. (1999). Differential temperature-dependent chaperone-like activity of alphaA-  
674 and alphaB-crystallin homoaggregates. *J Biol Chem* *274*, 34773-34778. 10.1074/jbc.274.49.34773.
- 675 de Melo Reis, R.A., Ventura, A.L., Schitine, C.S., de Mello, M.C., and de Mello, F.G. (2008). Muller glia as  
676 an active compartment modulating nervous activity in the vertebrate retina: neurotransmitters and  
677 trophic factors. *Neurochem Res* *33*, 1466-1474. 10.1007/s11064-008-9604-1.
- 678 Dubin, R.A., Gopal-Srivastava, R., Wawrousek, E.F., and Piatigorsky, J. (1991). Expression of the murine  
679 alpha B-crystallin gene in lens and skeletal muscle: identification of a muscle-preferred enhancer. *Mol*  
680 *Cell Biol* *11*, 4340-4349. 10.1128/mcb.11.9.4340-4349.1991.
- 681 Dulle, J.E., and Fort, P.E. (2016). Crystallins and neuroinflammation: The glial side of the story. *Biochim*  
682 *Biophys Acta* *1860*, 278-286. 10.1016/j.bbagen.2015.05.023.
- 683 Fort, P.E., Freeman, W.M., Losiewicz, M.K., Singh, R.S., and Gardner, T.W. (2009). The retinal proteome  
684 in experimental diabetic retinopathy: up-regulation of crystallins and reversal by systemic and periocular  
685 insulin. *Mol Cell Proteomics* *8*, 767-779. 10.1074/mcp.M800326-MCP200.
- 686 Fu, S., Dong, S., Zhu, M., Sherry, D.M., Wang, C., You, Z., Haigh, J.J., and Le, Y.Z. (2015). Muller Glia Are a  
687 Major Cellular Source of Survival Signals for Retinal Neurons in Diabetes. *Diabetes* *64*, 3554-3563.  
688 10.2337/db15-0180.
- 689 Garcia, M., Forster, V., Hicks, D., and Vecino, E. (2002). Effects of muller glia on cell survival and  
690 neuritogenesis in adult porcine retina in vitro. *Invest Ophthalmol Vis Sci* *43*, 3735-3743.
- 691 Ghosh, K.S., and Chauhan, P. (2019). Crystallins and Their Complexes. *Subcell Biochem* *93*, 439-460.  
692 10.1007/978-3-030-28151-9\_14.
- 693 Heinig, N., Schumann, U., Calzia, D., Panfoli, I., Ader, M., Schmidt, M.H.H., Funk, R.H.W., and Roehlecke,  
694 C. (2020). Photobiomodulation Mediates Neuroprotection against Blue Light Induced Retinal  
695 Photoreceptor Degeneration. *Int J Mol Sci* *21*. 10.3390/ijms21072370.
- 696 Heise, E.A., Marozas, L.M., Grafton, S.A., Green, K.M., Kirwin, S.J., and Fort, P.E. (2013). Strain-  
697 independent increases of crystallin proteins in the retina of type 1 diabetic rats. *PLoS One* *8*, e82520.  
698 10.1371/journal.pone.0082520.
- 699 Hejtmancik, J.F., Riazuddin, S.A., McGreal, R., Liu, W., Cvekl, A., and Shiels, A. (2015). Lens Biology and  
700 Biochemistry. *Prog Mol Biol Transl Sci* *134*, 169-201. 10.1016/bs.pmbts.2015.04.007.
- 701 Hicks, D., and Courtois, Y. (1990). The growth and behaviour of rat retinal Muller cells in vitro. 1. An  
702 improved method for isolation and culture. *Exp Eye Res* *51*, 119-129. 10.1016/0014-4835(90)90063-z.

- 703 Horwitz, J. (1992). Alpha-crystallin can function as a molecular chaperone. *Proc Natl Acad Sci U S A* *89*,  
704 10449-10453. 10.1073/pnas.89.21.10449.
- 705 Horwitz, J., Bova, M.P., Ding, L.L., Haley, D.A., and Stewart, P.L. (1999). Lens alpha-crystallin: function  
706 and structure. *Eye (Lond)* *13 ( Pt 3b)*, 403-408. 10.1038/eye.1999.114.
- 707 Hua Wang, Y., Wu Wang, D., and Qin Yin, Z. (2020). Synergistic protection of RGCs by olfactory  
708 ensheathing cells and alpha-crystallin through regulation of the Akt/BAD Pathway. *J Fr Ophthalmol* *43*,  
709 718-726. 10.1016/j.jfo.2020.02.003.
- 710 Jeong, W.J., Rho, J.H., Yoon, Y.G., Yoo, S.H., Jeong, N.Y., Ryu, W.Y., Ahn, H.B., Park, W.C., Rho, S.H., Yoon,  
711 H.S., et al. (2012). Cytoplasmic and nuclear anti-apoptotic roles of alphaB-crystallin in retinal pigment  
712 epithelial cells. *PLoS One* *7*, e45754. 10.1371/journal.pone.0045754.
- 713 Kannan, R., Sreekumar, P.G., and Hinton, D.R. (2016). Alpha crystallins in the retinal pigment epithelium  
714 and implications for the pathogenesis and treatment of age-related macular degeneration. *Biochim*  
715 *Biophys Acta* *1860*, 258-268. 10.1016/j.bbagen.2015.05.016.
- 716 Kase, S., Meghpara, B.B., Ishida, S., and Rao, N.A. (2012). Expression of alpha-crystallin in the retina of  
717 human sympathetic ophthalmia. *Mol Med Rep* *5*, 395-399. 10.3892/mmr.2011.653.
- 718 Kim, Y.H., Choi, M.Y., Kim, Y.S., Han, J.M., Lee, J.H., Park, C.H., Kang, S.S., Choi, W.S., and Cho, G.J. (2007).  
719 Protein kinase C delta regulates anti-apoptotic alphaB-crystallin in the retina of type 2 diabetes.  
720 *Neurobiol Dis* *28*, 293-303. 10.1016/j.nbd.2007.07.017.
- 721 Lee, S.W., Rho, J.H., Lee, S.Y., Yoo, S.H., Kim, H.Y., Chung, W.T., and Yoo, Y.H. (2016). Alpha B-Crystallin  
722 Protects Rat Articular Chondrocytes against Casein Kinase II Inhibition-Induced Apoptosis. *PLoS One* *11*,  
723 e0166450. 10.1371/journal.pone.0166450.
- 724 Liu, J.P., Schlosser, R., Ma, W.Y., Dong, Z., Feng, H., Liu, L., Huang, X.Q., Liu, Y., and Li, D.W. (2004).  
725 Human alphaA- and alphaB-crystallins prevent UVA-induced apoptosis through regulation of PKCalpha,  
726 RAF/MEK/ERK and AKT signaling pathways. *Exp Eye Res* *79*, 393-403. 10.1016/j.exer.2004.06.015.
- 727 Losiewicz, M.K., and Fort, P.E. (2011). Diabetes impairs the neuroprotective properties of retinal alpha-  
728 crystallins. *Invest Ophthalmol Vis Sci* *52*, 5034-5042. iovs.10-6931 [pii]  
729 10.1167/iov.10-6931.
- 730 MacRae, T.H. (2000). Structure and function of small heat shock/alpha-crystallin proteins: established  
731 concepts and emerging ideas. *Cell Mol Life Sci* *57*, 899-913. 10.1007/pl00000733.
- 732 Makley, L.N., McMenimen, K.A., DeVree, B.T., Goldman, J.W., McGlasson, B.N., Rajagopal, P., Dunyak,  
733 B.M., McQuade, T.J., Thompson, A.D., Sunahara, R., et al. (2015). Pharmacological chaperone for alpha-  
734 crystallin partially restores transparency in cataract models. *Science* *350*, 674-677.  
735 10.1126/science.aac9145.
- 736 Masilamoni, J.G., Jesudason, E.P., Bharathi, S.N., and Jayakumar, R. (2005). The protective effect of  
737 alpha-crystallin against acute inflammation in mice. *Biochim Biophys Acta* *1740*, 411-420.  
738 10.1016/j.bbadis.2004.11.002.
- 739 Morrison, L.E., Hoover, H.E., Thuerauf, D.J., and Glembotski, C.C. (2003). Mimicking phosphorylation of  
740 alphaB-crystallin on serine-59 is necessary and sufficient to provide maximal protection of cardiac  
741 myocytes from apoptosis. *Circ Res* *92*, 203-211. 10.1161/01.res.0000052989.83995.a5.
- 742 Munemasa, Y., Kwong, J.M., Caprioli, J., and Piri, N. (2009). The role of alphaA- and alphaB-crystallins in  
743 the survival of retinal ganglion cells after optic nerve axotomy. *Invest Ophthalmol Vis Sci* *50*, 3869-3875.  
744 10.1167/iov.08-3138.
- 745 Nath, M., Shan, Y., Myers, A.M., and Fort, P.E. (2021). HspB4/alphaA-Crystallin Modulates  
746 Neuroinflammation in the Retina via the Stress-Specific Inflammatory Pathways. *J Clin Med* *10*.  
747 10.3390/jcm10112384.

- 748 Pasupuleti, N., Matsuyama, S., Voss, O., Doseff, A.I., Song, K., Danielpour, D., and Nagaraj, R.H. (2010).  
749 The anti-apoptotic function of human alphaA-crystallin is directly related to its chaperone activity. *Cell*  
750 *Death Dis* 1, e31. 10.1038/cddis.2010.3.
- 751 Pereiro, X., Miltner, A.M., La Torre, A., and Vecino, E. (2020). Effects of Adult Muller Cells and Their  
752 Conditioned Media on the Survival of Stem Cell-Derived Retinal Ganglion Cells. *Cells* 9.  
753 10.3390/cells9081759.
- 754 Piri, N., Kwong, J.M., and Caprioli, J. (2013). Crystallins in retinal ganglion cell survival and regeneration.  
755 *Mol Neurobiol* 48, 819-828. 10.1007/s12035-013-8470-2.
- 756 Piri, N., Kwong, J.M., Gu, L., and Caprioli, J. (2016). Heat shock proteins in the retina: Focus on HSP70  
757 and alpha crystallins in ganglion cell survival. *Prog Retin Eye Res* 52, 22-46.  
758 10.1016/j.preteyeres.2016.03.001.
- 759 Rao, C.M., Raman, B., Ramakrishna, T., Rajaraman, K., Ghosh, D., Datta, S., Trivedi, V.D., and  
760 Sukhaswami, M.B. (1998). Structural perturbation of alpha-crystallin and its chaperone-like activity. *Int J*  
761 *Biol Macromol* 22, 271-281. 10.1016/s0141-8130(98)00025-7.
- 762 Rao, N.A., Saraswathy, S., Wu, G.S., Katselis, G.S., Wawrousek, E.F., and Bhat, S. (2008). Elevated retina-  
763 specific expression of the small heat shock protein, alphaA-crystallin, is associated with photoreceptor  
764 protection in experimental uveitis. *Invest Ophthalmol Vis Sci* 49, 1161-1171. 49/3/1161 [pii]  
765 10.1167/iovs.07-1259.
- 766 Reddy, G.B., Kumar, P.A., and Kumar, M.S. (2006). Chaperone-like activity and hydrophobicity of alpha-  
767 crystallin. *IUBMB Life* 58, 632-641. 10.1080/15216540601010096.
- 768 Reddy, V.S., Raghu, G., Reddy, S.S., Pasupulati, A.K., Suryanarayana, P., and Reddy, G.B. (2013).  
769 Response of small heat shock proteins in diabetic rat retina. *Invest Ophthalmol Vis Sci* 54, 7674-7682.  
770 10.1167/iovs.13-12715.
- 771 Robinson, M.L., and Overbeek, P.A. (1996). Differential expression of alpha A- and alpha B-crystallin  
772 during murine ocular development. *Invest Ophthalmol Vis Sci* 37, 2276-2284.
- 773 Rodriguez, A.R., de Sevilla Muller, L.P., and Brecha, N.C. (2014). The RNA binding protein RBPMS is a  
774 selective marker of ganglion cells in the mammalian retina. *J Comp Neurol* 522, 1411-1443.  
775 10.1002/cne.23521.
- 776 Rubsam, A., Parikh, S., and Fort, P.E. (2018). Role of Inflammation in Diabetic Retinopathy. *Int J Mol Sci*  
777 19. 10.3390/ijms19040942.
- 778 Ruebsam, A., Dulle, J.E., Myers, A.M., Sakrikar, D., Green, K.M., Khan, N.W., Schey, K., and Fort, P.E.  
779 (2018). A specific phosphorylation regulates the protective role of alphaA-crystallin in diabetes. *JCI*  
780 *Insight* 3. 10.1172/jci.insight.97919.
- 781 Schmidt, T., Bartelt-Kirbach, B., and Golenhofen, N. (2012). Phosphorylation-dependent subcellular  
782 localization of the small heat shock proteins HspB1/Hsp25 and HspB5/alphaB-crystallin in cultured  
783 hippocampal neurons. *Histochem Cell Biol* 138, 407-418. 10.1007/s00418-012-0964-x.
- 784 Schneider, C.A., Rasband, W.S., and Eliceiri, K.W. (2012). NIH Image to ImageJ: 25 years of image  
785 analysis. *Nature Methods* 9, 671-675. 10.1038/nmeth.2089.
- 786 Shao, W.Y., Liu, X., Gu, X.L., Ying, X., Wu, N., Xu, H.W., and Wang, Y. (2016). Promotion of axon  
787 regeneration and inhibition of astrocyte activation by alpha A-crystallin on crushed optic nerve. *Int J*  
788 *Ophthalmol* 9, 955-966. 10.18240/ijo.2016.07.04.
- 789 Shi, Y., Su, C., Wang, J.T., Du, B., Dong, L.J., Liu, A.H., and Li, X.R. (2015). Temporal and spatial changes in  
790 VEGF, alphaA- and alphaB-crystallin expression in a mouse model of oxygen-induced retinopathy. *Int J*  
791 *Clin Exp Med* 8, 3349-3359.
- 792 Takemoto, L.J. (1996). Differential phosphorylation of alpha-A crystallin in human lens of different age.  
793 *Exp Eye Res* 62, 499-504. 10.1006/exer.1996.0060.



794 Teodorowicz, M., Perdijk, O., Verhoek, I., Govers, C., Savelkoul, H.F.J., Tang, Y., Wichers, H., and  
795 Broersen, K. (2017). Optimized Triton X-114 assisted lipopolysaccharide (LPS) removal method reveals  
796 the immunomodulatory effect of food proteins. *PLOS ONE* *12*, e0173778.  
797 10.1371/journal.pone.0173778.

798 Vecino, E., Rodriguez, F.D., Ruzafa, N., Pereiro, X., and Sharma, S.C. (2016). Glia-neuron interactions in  
799 the mammalian retina. *Prog Retin Eye Res* *51*, 1-40. 10.1016/j.preteyeres.2015.06.003.

800 Wang, Y.H., Wang, D.W., Wu, N., Wang, Y., and Yin, Z.Q. (2011). Alpha-crystallin promotes rat retinal  
801 neurite growth on myelin substrates in vitro. *Ophthalmic Res* *45*, 164-168. 10.1159/000319944.

802 Winzeler, A., and Wang, J.T. (2013). Purification and culture of retinal ganglion cells from rodents. *Cold*  
803 *Spring Harb Protoc* *2013*, 643-652. 10.1101/pdb.prot074906.

804 Yaung, J., Kannan, R., Wawrousek, E.F., Spee, C., Sreekumar, P.G., and Hinton, D.R. (2008). Exacerbation  
805 of retinal degeneration in the absence of alpha crystallins in an in vivo model of chemically induced  
806 hypoxia. *Exp Eye Res* *86*, 355-365. S0014-4835(07)00323-5 [pii]  
807 10.1016/j.exer.2007.11.007.

808 Ying, X., Peng, Y., Zhang, J., Wang, X., Wu, N., Zeng, Y., and Wang, Y. (2014). Endogenous alpha-crystallin  
809 inhibits expression of caspase-3 induced by hypoxia in retinal neurons. *Life Sci* *111*, 42-46.  
810 10.1016/j.lfs.2014.07.008.

811 Ying, X., Zhang, J., Wang, Y., Wu, N., Wang, Y., and Yew, D.T. (2008). Alpha-crystallin protected axons  
812 from optic nerve degeneration after crushing in rats. *J Mol Neurosci* *35*, 253-258. 10.1007/s12031-007-  
813 9010-1.

814 Zhang, J., Liu, J., Wu, J., Li, W., Chen, Z., and Yang, L. (2019). Progression of the role of CRYAB in signaling  
815 pathways and cancers. *Onco Targets Ther* *12*, 4129-4139. 10.2147/OTT.S201799.

816 Zhu, Z., and Reiser, G. (2018). The small heat shock proteins, especially HspB4 and HspB5 are promising  
817 protectants in neurodegenerative diseases. *Neurochem Int* *115*, 69-79. 10.1016/j.neuint.2018.02.006.

818

819

820 Table 1: Primers used for point mutations on T148 corresponding to the phosphomimetic (T148D) and  
821 the non-phosphorylatable (T148A) analogue of  $\alpha$ A-crystallin.

822

Protein	Primers
T148A	5'-gcatccaggccagcctggatcttgggg-3' 5'-ccccaagatccaggctggcctggatgc-3'
T148D	5'-gtggcatccaggccatcctggatcttggggcc-3' 5'-ggccccaagatccaggatggcctggatgccac-3'

823

824

